


---


# DOE2VEC: DEEP-LEARNING BASED FEATURES FOR EXPLORATORY LANDSCAPE ANALYSIS


---

**Bas van Stein**   
LIACS, Leiden University  
Leiden, The Netherlands  
b.van.stein@liacs.leidenuniv.nl

**Fu Xing Long**   
BMW Group  
Munich, Germany  
fu-xing.long@bmw.de

**Moritz Frenzel**   
BMW Group  
Munich, Germany  
moritz.frenzel@bmw.de

**Peter Krause**   
divis intelligent solutions GmbH  
Dortmund, Germany  
krause@divis-gmbh.de

**Markus Gitterle**   
University of Applied Sciences Munich  
Munich, Germany  
markus.gitterle@hm.edu

**Thomas Bäck**   
LIACS, Leiden University  
Leiden, The Netherlands  
t.h.w.baeck@liacs.leidenuniv.nl

## ABSTRACT

We propose DoE2Vec, a variational autoencoder (VAE)-based methodology to learn optimization landscape characteristics for downstream meta-learning tasks, e.g., automated selection of optimization algorithms. Principally, using large training data sets generated with a random function generator, DoE2Vec self-learns an informative latent representation for any design of experiments (DoE). Unlike the classical exploratory landscape analysis (ELA) method, our approach does not require any feature engineering and is easily applicable for high dimensional search spaces. For validation, we inspect the quality of latent reconstructions and analyze the latent representations using different experiments. The latent representations not only show promising potentials in identifying similar (cheap-to-evaluate) surrogate functions, but also can significantly boost performances when being used complementary to the classical ELA features in classification tasks.

**Keywords** exploratory landscape analysis, landscape features, auto-encoders, optimization

## 1 Introduction

Solving real-world black-box optimization problems can be extremely complicated, particularly if they are strongly nonlinear and require expensive function evaluations. As suggested by the no free lunch theorem in [1], there is no such things as a single-best optimization algorithm, that is capable of optimally solving all kind of problems. The task in identifying the most time- and resource-efficient optimization algorithms for each specific problem, also known as the algorithm selection problem (ASP) (see [2]), is tedious and challenging, even with domain knowledge and experience. In recent years, landscape-aware algorithm selection has gained increasing attention from the research community, where the fitness landscape characteristics are exploited to explain the effectiveness of an algorithm across different problem instances (see [3, 4]). Beyond that, it has been shown that landscape characteristics are sufficiently informative in reliably predicting the performance of optimization algorithms, e.g., using Machine Learning approaches (see [5–10]). In other words, the expected performance of an optimization algorithm on an unseen problem can be estimated, once the corresponding landscape characteristics have been identified. Interested readers are referred to [7, 11–14].

Exploratory landscape analysis (ELA), for instance, considers six classes of expertly designed features, including  $y$ -distribution, level set, meta-model, local search, curvature and convexity, to numerically quantify the landscape

complexity of an optimization problem, such as multimodality, global structure, separability, plateaus, etc. (see [15, 16]). Each feature class consists of a set of features, which can be relatively cheaply computed. Other than typical ASP tasks, ELA has shown great potential in a wide variety of applications, such as understanding the underlying landscape of neural architecture search problems in [17] and classifying the Black-Box Optimization Benchmarking (BBOB) problems in [18]. Recently, ELA has been applied not only to analyze the landscape characteristics of crash-worthiness optimization problems from automotive industry, but also to identify appropriate cheap-to-evaluate functions as representative of the expensive real-world problems (see [19]). While ELA is well established in capturing the optimization landscape characteristics, we would like to raise our concerns regarding the following aspects.

1. Many of the ELA features are highly correlated and redundant, particularly those within the same feature class (see [20]).
2. Some of the ELA features are insufficiently expressive in distinguishing problem instances (see [21]).
3. Since ELA features are manually engineered by experts, their feature computation might be biased in capturing certain landscape characteristics (see [22]).
4. ELA features are less discriminative for high-dimensional problems (see [23]).

Instead of improving the ELA method directly, e.g., searching for more discriminative landscape features, we approach the problems from a different perspective. In this paper, we introduce an automated self-supervised representation learning approach to characterize optimization landscapes by exploiting information in the latent space. Essentially, a deep variational autoencoder (VAE) model is trained to extract an informative feature vector from a design of experiments (DoE), which is essentially a generic low-dimensional representation of the optimization landscape. Thus, the name of our approach: *DoE2Vec*. While the functionality of our approach is fully independent of ELA, experimental results reveal that its performance can be further improved when combined with ELA (and vice versa). To the best of our knowledge, a similar application approach with VAE in learning optimization landscape characteristics is still lacking. Section 2 briefly introduces the state-of-the-art representation learning of optimization landscapes as well as the concepts of (variational) autoencoder. This is followed by the description of our methodology in Section 3. Next, we explain and discuss our experimental results in Section 4. Lastly, conclusions and outlooks are included in Section 5.

## 2 Representation of Optimization Landscape

In the conventional ELA approach, landscape features are computed primarily using a DoE of some samples points  $\mathcal{W} = \{w_1, \dots, w_n\}$  evaluated on an objective function  $f$ , i.e.,  $f: \mathbb{R}^d \rightarrow \mathbb{R}$ , with  $w_i \in \mathbb{R}^d$ ,  $n$  represents sample size, and  $d$  represents function dimension. The objective function values  $f(w_i)$ ,  $i \in \{1, \dots, n\}$  are the inputs of VAE models in DoE2Vec. In this work, we consider ELA features similar to those in [19], which do not require additional sampling, and compute them with the package `f1acco` by [24, 25]. These features include commonly used dimensionality reduction approaches such as Principal Component Analysis (PCA) [26], a number of simple surrogate models and many others.

To overcome the drawbacks of the ELA approach, attentions have been focused on developing algorithm selection approaches without requiring landscape features. For example, [27] proposed two feature-free approaches using a deep learning method, where optimization landscapes can be represented through either 1) image-based fitness maps or 2) graph-like fitness clouds. In the first approach, convolutional neural networks were employed to project data sets into two-dimensional fitness maps, using different dimensionality reduction techniques. In the second approach, data sets were embedded into point clouds using modified point cloud transformers, which can accurately capture the global landscape characteristics. Nonetheless, the fitness map approach suffered from the curse of dimensionality, while the fitness cloud approach was limited to fixed training sample size. Additional relevant works can be found in [22, 28–30]. Unlike these approaches, which were directly used as classifiers, the latent feature sets generated by our proposed approach can be easily combined with other features, such as ELA features, for classification tasks. In our work, we do not propose to replace conventional ELA features, but to actually extend them with autoencoder (AE) based latent-space features. Since the implementation of both approaches mentioned above is not available, a comparison to our work in terms of classifying high-level properties is only feasible by directly comparing their results on a identical experimental setup. Following this, results from the downstream tasks in this work can partially be compared to the mentioned results in [29], including the standard Principal Component Analysis (PCA), reduced Multiple Channel (rMC) and a transformer based approach (Transf.), taking into account that additional hyperparameter tuning was involved in their classification experiments with ELA features.

Our approach is capable of learning the representations of optimization landscapes in an automated, generic and unsupervised manner, with the advantage that the learned features are not biased towards any particular landscape characteristic. Unlike previously mentioned approaches, our proposed method is independent of the sampling method. By using only fully connected (dense) layers that learn from one-dimensional (flattened) landscapes, an AE or a VAE is,

in theory, capable of learning any number of input-dimensions without scaling difficulties. Furthermore, the fast-to-train (V)AE models can be easily shared in practice.

## 2.1 Autoencoder

A standard AE usually has a symmetrical architecture, consisting of three components: an encoder, a hidden layer, also known as bottleneck, and a decoder (Figure 1). In short, an encoder projects the input space  $\mathcal{X}$  to a representative feature space  $\mathcal{H}$ , i.e.,  $e: \mathcal{X} \rightarrow \mathcal{H}$ , while a decoder transforms the feature space back to the input space  $d: \mathcal{H} \rightarrow \hat{\mathcal{X}}$  (see [31, 32]). In other words, AE attempts to optimally reconstruct the original input space  $\mathcal{X}$ , by minimizing the reconstruction error  $\mathcal{L}(\mathcal{X}, \hat{\mathcal{X}})$ , e.g. mean squared error, during the (unsupervised) training process. Commonly, AE is constructed with an input layer and an output layer of the same dimension  $\dim(X)$  and a bottleneck layer of lower dimension  $\dim(H)$ , i.e.,  $\dim(H) < \dim(X)$ , to improve its ability in capturing crucial representations of the input space.

Following this, AE has rapidly gained popularity in the field of dimensionality reduction as well as representation learning [33, 34]. In comparison with the simple principal component analysis (PCA) technique, AE has the advantage that nonlinear representation features can be learned with activation functions, such as a sigmoid function.

## 2.2 Variational autoencoder

Originating from the same family as traditional AE, a VAE typically has a similar architecture with some modifications, as shown in Figure 1. Unlike AE, the latent space of a VAE is encoded as a distribution by using a mean and variance

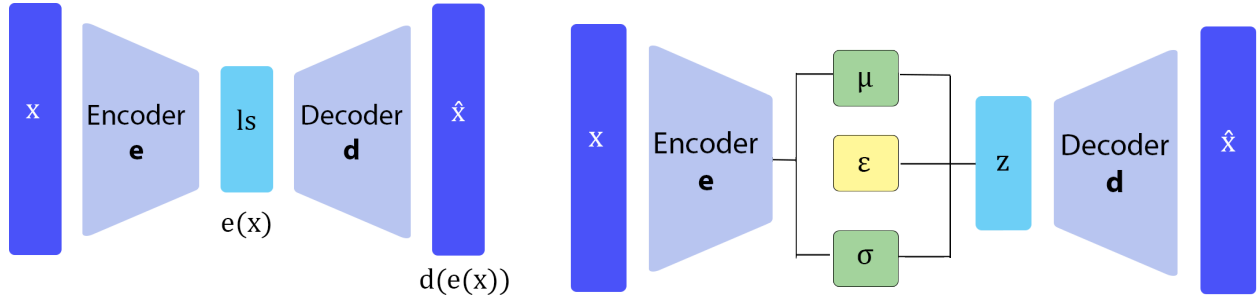


Figure 1: Architecture of a (standard) AE on the left and VAE on the right used in DoE2Vec. The latent space  $z$  is defined by  $z = \mu + \sigma \cdot \epsilon$ , where  $\epsilon$  denotes the sampling with mean  $\mu$  and variance  $\sigma$ .

layer, together with a sampling method. Following this, the latent space can be properly regularized to provide more meaningful features. During the training process, a common loss function  $\mathcal{L}_{\text{VAE}}$  (Equation 1) of VAE is to be minimized, consisting of a regularization term (Equation 2), which can be expressed as the Kullback–Leibler (KL) divergence  $\mathcal{L}_{\text{KL}}$ , and a reconstruction error, e.g., mean squared error  $\mathcal{L}_{\text{MSE}}$  (Equation 3).

$$\mathcal{L}_{\text{VAE}}(\mathcal{X}, \hat{\mathcal{X}}) = \beta \cdot \mathcal{L}_{\text{KL}}(\mathcal{X}, \hat{\mathcal{X}}) + \mathcal{L}_{\text{MSE}}(\mathcal{X}, \hat{\mathcal{X}}), \quad (1)$$

$$\mathcal{L}_{\text{KL}}(\mathcal{X}, \hat{\mathcal{X}}) = \frac{1}{2} \sum_{i=1}^{|\mathcal{X}|} (\exp(\sigma_i) - (1 + \sigma_i) + \mu_i^2), \quad (2)$$

$$\mathcal{L}_{\text{MSE}}(\mathcal{X}, \hat{\mathcal{X}}) = \sum_{x \in \mathcal{X}, \hat{x} \in \hat{\mathcal{X}}} (x - \hat{x})^2, \quad (3)$$

where a weighting factor  $\beta$  is included to ensure a good trade-off between  $\mathcal{L}_{\text{KL}}$  and  $\mathcal{L}_{\text{MSE}}$ ,  $\sigma$  and  $\mu$  are the variance and mean latent layers of the VAE and  $\hat{\mathcal{X}}$  is the reconstruction of the input space. Detailed explanations regarding VAE can be found in [35, 36].

## 2.3 Black-Box Optimization Benchmarking

The development of DoE2Vec is based on the well-known academic BBOB suite by [37], consisting of altogether 24 noise-free real-parameter single objective optimization problems of different landscape complexity. For each BBOB problem, the global optimum (within  $[-5, 5]^d$ ) can be randomly shifted, e.g., through translation or rotation, to generate a new problem instance.

### 3 Doe2Vec

Generally, our proposed method uses a VAE with similar design as described in Section 2.2. Precisely, our VAE model has an architecture of altogether seven fully connected layers, where rectified linear unit (ReLU) activation functions are assigned to the hidden layers, while a sigmoid activation function is used for the final output layer of the decoder. The encoder is composed of four fully connected layers with  $\dim(X)$  depending on the DoE sample size  $n$ , starting with the input layer size  $n$ , two hidden layers with sizes  $n/2$  and  $n/4$  and the latent size  $ls$  ( $ls < n/4$ ) for the mean and log variance of the latent space. The decoder is composed of three fully connected layers with sizes  $n/4$ ,  $n/2$  and  $n$  for the final output layer. The focus of our approach lies on VAE, rather than AE, because it has the additional benefits of regularizing the latent space without loss of generalisation. For comparison, we consider a standard AE model as well (with the same number of hidden layers, except that the latent space is now a single dense layer, instead of a mean and log variance layer with a sampling scheme). Full specifications of the different models are available in our Github repository ([38]), while pre-trained models are also available on Huggingface.

The general workflow of DoE2Vec can be summarized as follows:

1. First, a DoE of size  $2^m$  is created, where  $m$  is a user defined parameter. By default, a Sobol sequence by [39] is used as sampling scheme, but any sampling scheme or even a custom DoE can be utilized in practice.
2. The DoE samples, initially within the domain  $[0, 1]^d$ , can be re-scaled to any desired function boundaries, as the DoE2Vec method is scale-invariant by design.
3. Next, the DoE samples are evaluated for a set of functions randomly generated using the random function generator from [19], which was originally proposed by [40]. The main advantage of using this function generator is that a large training set can be easily created, covering a wide range of function landscape of different complexity.
4. Following this, all objective function values are first re-scaled to  $[0, 1]$  and then used as input vectors to train (V)AE models.
5. Lastly, the latent space of the trained V(AE) models can be used as feature vectors for further downstream classification tasks, such as optimization algorithm selection.

In the next section, we will show that the learned feature representations have attractive characteristics and they are indeed useful for downstream classification and meta-learning tasks.

## 4 Experimental Results and Discussions

In this work, we have conducted altogether four experiments for different research purposes. Basically, the first two experiments are to investigate the quality of VAE models trained and to validate the latent space representation learned, while the last two experiments are to evaluate the potential of the DoE2Vec approach for downstream meta-learning tasks, as follows.

1. Analyzing the reconstruction of function landscapes and the impact of the latent size and KL loss weight (weighting factor  $\beta$ ).
2. Investigating the differences in latent space representation between a standard AE and a VAE model.
3. Identifying functions with similar landscapes based on the latent representations.
4. Three downstream multi-class classification experiment to show the potential of the proposed approach in practice, using the latent feature vectors as inputs.

In our experiments, we fix the sampling scheme to a Sobol sequence and  $m$  to eight, ending up with a DoE of 256 samples. Unless otherwise specified, all AE and VAE models are trained on a set of 250,000 five-dimensional ( $5d$ ) random functions.

### 4.1 Reconstruction of Function Landscapes

In our first experiment, we investigate the impact of two model parameters, namely the KL loss weight and the latent size, on the model loss functions. For this purpose, a total of 30 VAE models are trained using combinations of six different latent sizes (4, 8, 16, 24, 32) and five different KL loss weights (0.0001, 0.0002, 0.001, 0.005, 0.01). Results in the left subplot of Figure 2 clearly show that latent sizes have a positive effect on the  $\mathcal{L}_{\text{VAE}}$ , with the improvement

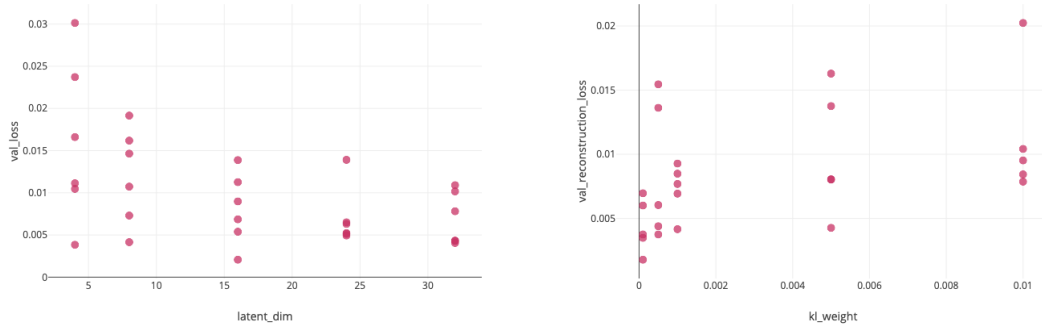


Figure 2: Impact of different latent sizes and KL loss weights on the loss functions. Left:  $\mathcal{L}_{VAE}$  against latent sizes. Right:  $\mathcal{L}_{MSE}$  against KL loss weight.

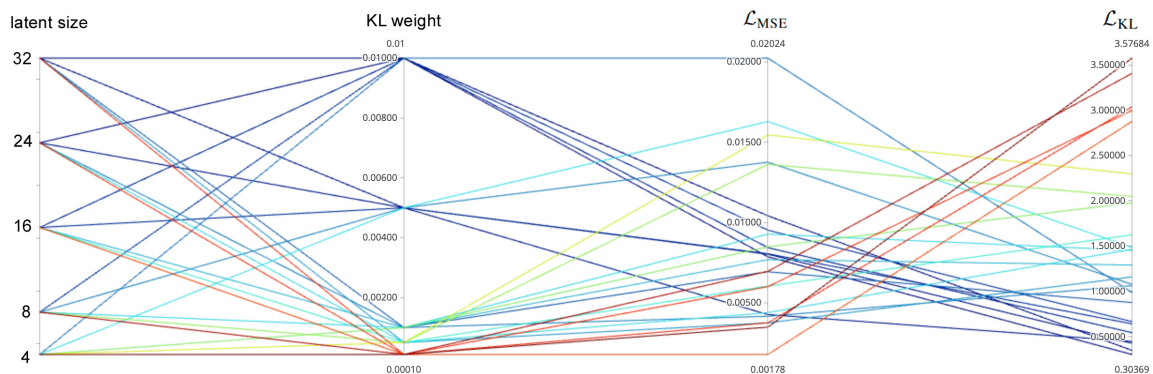


Figure 3: Parallel coordinates plot of different latent sizes and KL loss weights in relation with the validation  $\mathcal{L}_{KL}$  and  $\mathcal{L}_{MSE}$ . (Columns left to right: Latent size, KL loss weight,  $\mathcal{L}_{MSE}$  and  $\mathcal{L}_{KL}$ .) Each color or line represents a combination of latent size and KL loss weight. Conflict between both loss terms can be observed, since parameter combinations with low  $\mathcal{L}_{MSE}$  have a higher  $\mathcal{L}_{KL}$  and vice versa.

diminishes beyond 16. On the other hand, the  $\mathcal{L}_{MSE}$  can be improved with smaller KL loss weights, as shown in the right subplot. In Figure 3, the combined effects of these parameters on the  $\mathcal{L}_{KL}$  and  $\mathcal{L}_{MSE}$  are fully visualized.

In the remaining experiments, we use a latent size of either 24 or 32 (expressed as (V)AE-24 or (V)AE-32) and a KL loss weight of 0.001 as a good compromise between the two loss terms. It is to be noted that, while the (V)AE architecture can be further improved by applying neural architecture search, we leave it for future work, since the landscape reconstruction is not the ultimate purpose of this work. In fact, the reconstruction here is meant to be a way in evaluating the quality of learned representations. Subsequently, we verify the capability of a VAE-24 model by reconstructing a large variety of functions, using the 24 BBOB functions (first problem instance) (Figure 4).

## 4.2 Latent Space Representation

Next, we project the latent space of an AE and a VAE from our DoE2Vec approach onto a  $2d$  visualization using multidimensional scaling (MDS) method, as shown in Figure 5. For a comprehensive comparison, a similar MDS visualization for the feature vectors with all the (considered) ELA features is included as well. Interestingly, the latent space of ELA has a better looking cluster-structure, while the latent space of AE and VAE have a clear structure. As expected, the latent space of AE contains a few outliers and is in general more widespread than the latent space of VAE.

To further analyze the differences in latent space representation between the AE and VAE models, we use the generator part of the models to iteratively generate new function landscapes. To be precise, we select one latent representation as starting point and individually vary each latent variable with small steps between  $-1$  and  $+1$  of its original value. In Table 1, the generated landscapes are shown only for the extreme cases of an AE-4 and a VAE-4 model. Based on this result, two important conclusions can be drawn.

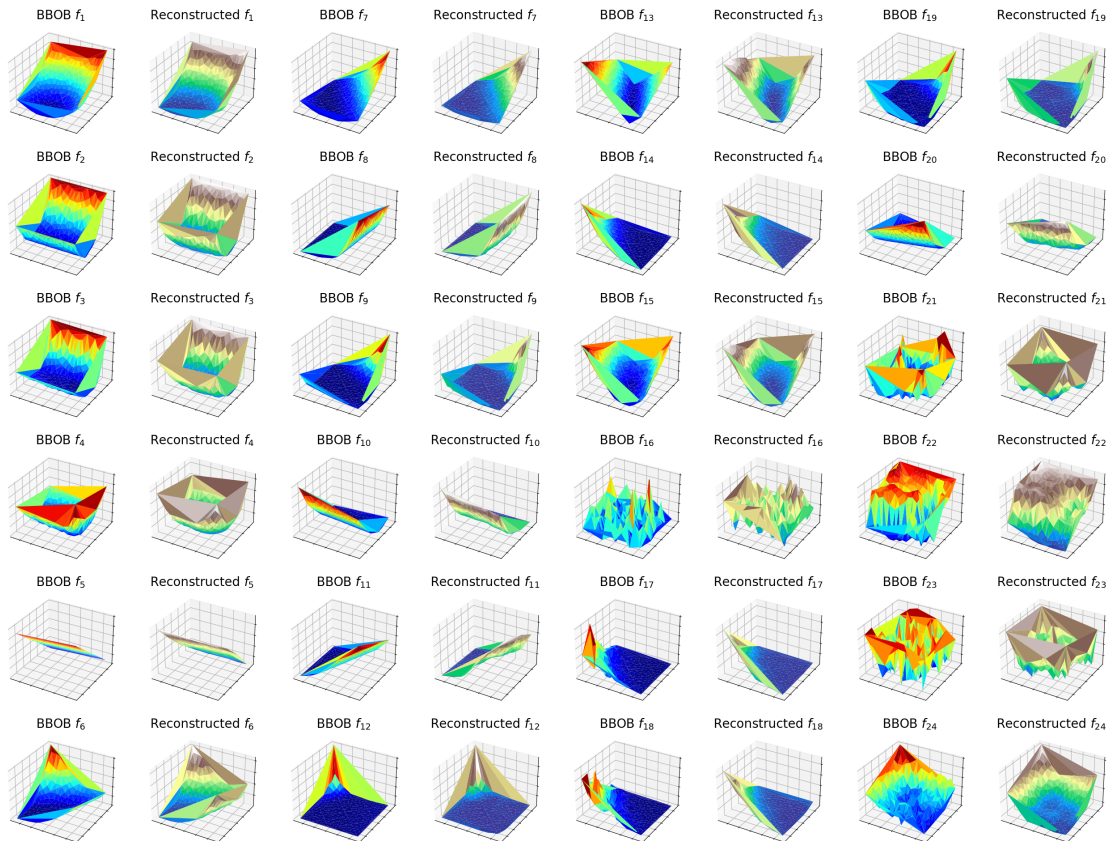


Figure 4: Reconstructions of the 24  $2d$  BBOB functions (labelled from  $f_1$  to  $f_{24}$ ) using a VAE-24 model. The surface plots are generated based on a DOE of 256 samples using triangulation. Generally, the reconstructed landscapes look similar to the actual landscapes based on visual inspection.

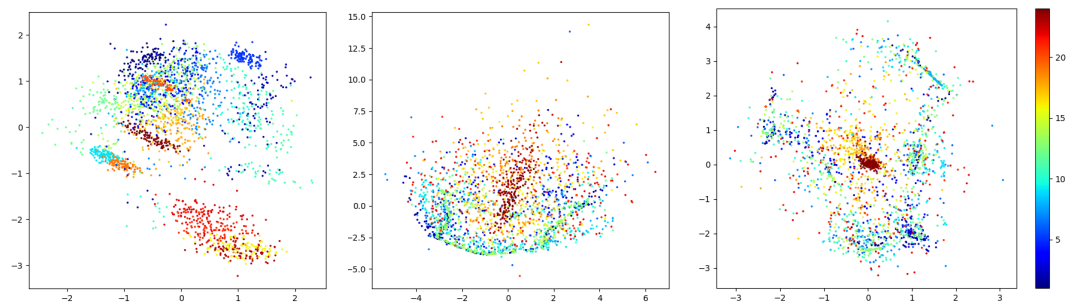
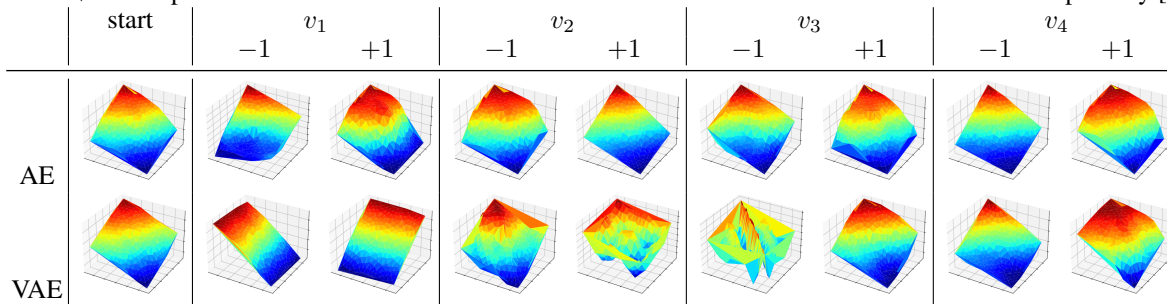


Figure 5: From left to right:  $2d$  MDS visualization of the (normalized) ELA feature spaces, the latent space of an AE-32 model and the latent space of a VAE-32 model. Altogether 100 problem instances for all 24 BBOB functions, resulting in a total of 2,400 dots (in each subplot), where each dot represents a feature vector of a BBOB instance and the color denotes the corresponding BBOB function.

1. The interpolation for both models is very smooth, showing that the models can learn the landscape representations well and are able to learn the structure, even though the dimensionality of the function landscapes  $d$  is not known.
2. The VAE model utilizes a more compact feature representation, where its output variance is greater than those of the AE model for the same variation of latent features.



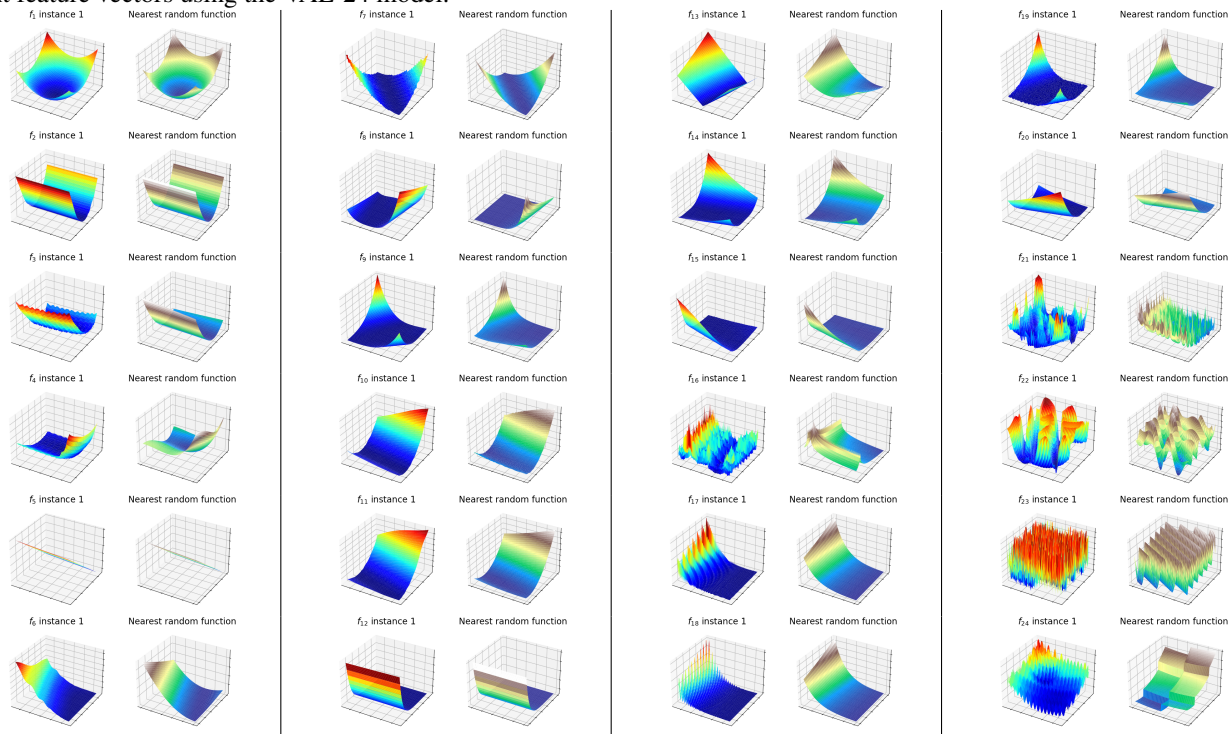
Table 1: Comparison of function landscapes generated by an AE-4 and a VAE-4 model for different latent variables, using the BBOB  $f_{22}$  encoding as starting point  $(v_1, v_2, v_3, v_4)$ . In each column, the latent features are separately varied by  $-1$  or  $+1$ . Complete variation of the latent features can be found in videos available in our Github repository [38].



### 4.3 Similar Representative Functions

The first main application of DoE2Vec is to identify cheap-to-evaluate functions with similar latent space representation for a given DoE, which can be very useful when dealing with real-world expensive black box optimization problems, as also described in [19]. In this way, large experiments can now be conducted on a “similar” function group at a much lower computational cost. Since a direct analytical verification of the results is very challenging, we instead use a visual inspection based on  $2d$  functions to showcase the potential of the proposed method. In Table 2, the 24 BBOB functions are paired with their respective “nearest” random function, where *nearest* is defined as the random function that has the closest feature representation in terms of Euclidean distance. For most BBOB functions, a very well fitting (almost identical) random function can be identified by the DoE2Vec model, where random functions of equal complexity are suggested for the more complex BBOB functions.

Table 2: Four columns with pairs of BBOB function and their respective nearest random function identified based on latent feature vectors using the VAE-24 model.



#### 4.4 Classification Tasks

Secondly, the DoE2Vec approach is designed to learn characteristic representations of an optimization landscape, which can be verified through a classical classification task of high level function properties. These high level properties, such as multimodality, global structure and funnel structure, are important for the ASP, as they often determine the difficulty of an optimization problem. Table 4 illustrates the BBOB functions and their associated high level properties.

Table 3: Classification results (averaged macro F1 scores over 10 runs with different random seeds) using a standard RF model with 100 trees, trained on the feature representations (from AE, VAE, classical ELA or ELA combined with VAE-32) of the first 100 instances for each BBOB function and validated on instance 101 to 120. \* PCA, rMC and Transformer results are directly taken from the work of [29], which uses an identical experimental setup but without repetitions.

| $d$ | Task           | AE-24        | AE-32        | VAE-24 | VAE-32 | ELA          | PCA*  | rMC*  | Transformer* | ELA-VAE-32   |
|-----|----------------|--------------|--------------|--------|--------|--------------|-------|-------|--------------|--------------|
| 2   | multimodal     | 0.875        | 0.849        | 0.877  | 0.856  | 0.984        | 0.994 | 0.971 | 0.991        | <b>0.991</b> |
|     | global struct. | 0.903        | 0.904        | 0.902  | 0.889  | 0.983        | 0.992 | 0.965 | 0.991        | <b>0.998</b> |
|     | funnel         | 0.985        | 0.974        | 0.956  | 0.978  | <b>1.000</b> | 0.999 | 0.995 | 1.000        | <b>1.000</b> |
| 5   | multimodal     | 0.908        | 0.903        | 0.880  | 0.889  | 0.963        | 0.897 | 0.947 | 0.991        | <b>0.998</b> |
|     | global struct. | 0.838        | 0.828        | 0.810  | 0.793  | <b>1.000</b> | 0.807 | 0.859 | 0.978        | <b>1.000</b> |
|     | funnel         | <b>1.000</b> | <b>1.000</b> | 0.996  | 0.991  | <b>1.000</b> | 0.990 | 0.989 | 1.000        | <b>1.000</b> |
| 10  | multimodal     | 0.877        | 0.813        | 0.844  | 0.838  | <b>1.000</b> | 0.839 | 0.952 | 0.974        | <b>1.000</b> |
|     | global struct. | 0.794        | 0.737        | 0.783  | 0.745  | 0.902        | 0.774 | 0.911 | 0.963        | <b>0.991</b> |
|     | funnel         | 0.998        | 0.993        | 0.997  | 0.993  | 0.972        | 0.977 | 0.991 | <b>1.000</b> | 0.997        |
| 20  | multimodal     | 0.726        | 0.722        | 0.700  | 0.694  | 0.970        | -     | -     | -            | <b>0.991</b> |
|     | global struct. | 0.689        | 0.621        | 0.606  | 0.626  | 0.972        | -     | -     | -            | <b>0.997</b> |
|     | funnel         | 0.993        | 0.982        | 0.985  | 0.982  | <b>1.000</b> | -     | -     | -            | <b>1.000</b> |

Table 4: High level properties of the 24 BBOB functions. This table was first introduced in [29]

| BBOB function                  | Multimodal | Global Structure | Funnel |
|--------------------------------|------------|------------------|--------|
| 1: Sphere                      | none       | none             | yes    |
| 2: Ellipsoidal separable       | none       | none             | yes    |
| 3: Rastrigin separable         | high       | strong           | yes    |
| 4: Büche-Rastrigin             | high       | strong           | yes    |
| 5: Linear Slope                | none       | none             | yes    |
| 6: Attractive Sector           | none       | none             | yes    |
| 7: Step Ellipsoidal            | none       | none             | yes    |
| 8: Rosenbrock                  | low        | none             | yes    |
| 9: Rosenbrock rotated          | low        | none             | yes    |
| 10: Ellipsoidal high cond.     | none       | none             | yes    |
| 11: Discus                     | none       | none             | yes    |
| 12: Bent Cigar                 | none       | none             | yes    |
| 13: Sharp Ridge                | none       | none             | yes    |
| 14: Different Powers           | none       | none             | yes    |
| 15: Rastrigin multimodal       | high       | strong           | yes    |
| 16: Weierstrass                | high       | medium           | none   |
| 17: Schaffer F7                | high       | medium           | yes    |
| 18: Schaffer F7 mod. ill-cond. | high       | medium           | yes    |
| 19: Griewank-Rosenbrock        | high       | strong           | yes    |
| 20: Schwefel                   | medium     | deceptive        | yes    |
| 21: Gallagher 101 Peaks        | medium     | none             | none   |
| 22: Gallagher 21 Peaks         | low        | none             | none   |
| 23: Katsuura                   | high       | none             | none   |
| 24: Lunacek bi-Rastrigin       | high       | weak             | yes    |

In this experiment, a standard random forest (RF) model (using `sklearn` from [41]) is implemented for the multiclass classification tasks based on the latent representations learned by four DoE2Vec models, consisting of AE-24, AE-32,



VAE-24 and VAE-32. In other words, the high level properties of a BBOB function are to be predicted using the latent representations. Again, we compare the DoE2Vec approach against the classical ELA method, which is specifically constructed to excel in exactly this kind of function property classification tasks. Beyond that, a combination of classical ELA features with a VAE-32 model is included to evaluate the complimentary effect of the different feature sets.

The classification results (macro F1 scores) of the different feature sets are summarized in Table 3. It is not surprising that the ELA features generally perform very well and outperform the latent features most of the time, especially in classifying the global structure and multimodal landscapes. Fascinatingly, the classification performances can be significantly improved when the DoE2Vec is combined with the classical ELA method, indicating that both feature sets seem to be complimentary to each other.

## 5 Conclusions and Future Work

In this work we propose *DoE2Vec*, a VAE-based approach to learn the latent representations of an optimization landscape, similar to the classical landscape features. Using a wide set of experiments, we have shown that DoE2Vec is able to reconstruct a large set of functions accurately and that the approach can be used for downstream meta-learning tasks, such as algorithm selection. The proposed methodology can be effectively used next to existing techniques, such as classical ELA features, to further increase the classification accuracy of certain downstream tasks. In fact, DoE2Vec can learn good feature representations for optimization landscapes and has several advantages over the ELA approach, such as feature engineering or selection knowledge is not required, domain knowledge in ELA is not needed and it is applicable to optimization tasks in a very straightforward manner. Nonetheless, there are a few known limitations to the proposed method, such as 1) Our approach is scale-invariant, but not rotation- or translation-invariant. Using a different loss function to train the autoencoders might be able to improve this 2) If a custom DoE sample is used, the model needs to be trained from scratch (no pre-trained model available). This typically takes a few minutes up to an hour, depending on the sample size  $n$  and number of random functions to train on, 3) The learned feature representations are a black-box that are hard to interpret directly.

In future work, we plan to improve our approach by tackling some of the challenges mentioned. Apart from that, we would like to verify the usefulness of the random functions with similar latent features w.r.t. the performances of an optimization algorithm.

## 6 Reproducibility statement

We provide an open-source documented implementation of our package at [38], with visualizations and video explanations. Pre-trained models (weights) are available on Huggingface. All models are trained using a single T4 GPU and the computations are carbon neutral ( $CO_2$ -free) by using solar power. Average training time of a model on 250,000 random functions was five minutes.

## References

- [1] David H. Wolpert and William G. Macready. No free lunch theorems for optimization. *IEEE Transactions on Evolutionary Computation*, 1(1):67–82, 1997.
- [2] John R. Rice. The algorithm selection problem. volume 15 of *Advances in Computers*, pages 65–118. Elsevier, 1976.
- [3] Bas van Stein, Michael Emmerich, and Zhiwei Yang. Fitness landscape analysis of nk landscapes and vehicle routing problems by expanded barrier trees. In *EVOLVE-A Bridge between Probability, Set Oriented Numerics, and Evolutionary Computation IV*, pages 75–89. Springer, 2013.
- [4] David Simoncini, Sophie Barbe, Thomas Schiex, and Sébastien Verel. Fitness landscape analysis around the optimum in computational protein design. In *Proceedings of the Genetic and Evolutionary Computation Conference, GECCO '18*, page 355–362, New York, NY, USA, 2018. Association for Computing Machinery.
- [5] Bernd Bischl, Olaf Mersmann, Heike Trautmann, and Mike Preuß. Algorithm selection based on exploratory landscape analysis and cost-sensitive learning. In *Proceedings of the 14th Annual Conference on Genetic and Evolutionary Computation, GECCO '12*, page 313–320, New York, NY, USA, 2012. Association for Computing Machinery.
- [6] Johann Dréo, Carola Doerr, and Yann Semet. Coupling the design of benchmark with algorithm in landscape-aware solver design. In *Proceedings of the Genetic and Evolutionary Computation Conference Companion, GECCO '19*, page 1419–1420, New York, NY, USA, 2019. Association for Computing Machinery.

- [7] Pascal Kerschke and Heike Trautmann. Automated algorithm selection on continuous black-box problems by combining exploratory landscape analysis and machine learning. *Evolutionary Computation*, 27(1):99–127, 2019.
- [8] Anja Jankovic and Carola Doerr. Landscape-aware fixed-budget performance regression and algorithm selection for modular cma-es variants. In *Proceedings of the 2020 Genetic and Evolutionary Computation Conference*, GECCO '20, page 841–849, New York, NY, USA, 2020. Association for Computing Machinery.
- [9] Anja Jankovic, Gorjan Popovski, Tome Eftimov, and Carola Doerr. *The Impact of Hyper-Parameter Tuning for Landscape-Aware Performance Regression and Algorithm Selection*, page 687–696. GECCO '21. Association for Computing Machinery, New York, NY, USA, 2021.
- [10] Maxim Pikalov and Vladimir Mironovich. *Automated Parameter Choice with Exploratory Landscape Analysis and Machine Learning*, page 1982–1985. GECCO '21. Association for Computing Machinery, New York, NY, USA, 2021.
- [11] Mario Andrés Muñoz, Yuan Sun, Michael Kirley, and Saman K. Halgamuge. Algorithm selection for black-box continuous optimization problems: A survey on methods and challenges. *Information Sciences*, 317:224–245, 2015.
- [12] Mario Andrés Muñoz, Michael Kirley, and Saman K. Halgamuge. Exploratory landscape analysis of continuous space optimization problems using information content. *IEEE Transactions on Evolutionary Computation*, 19(1):74–87, 2015.
- [13] Pascal Kerschke, Holger Hoos, Frank Neumann, and Heike Trautmann. Automated algorithm selection: Survey and perspectives. *Evolutionary Computation*, 27(1):3–45, 2019.
- [14] Katherine Mary Malan. A survey of advances in landscape analysis for optimisation. *Algorithms*, 14(2):40, 2021.
- [15] Olaf Mersmann, Mike Preuss, and Heike Trautmann. Benchmarking evolutionary algorithms: Towards exploratory landscape analysis. In Robert Schaefer, Carlos Cotta, Joanna Kołodziej, and Günter Rudolph, editors, *Parallel Problem Solving from Nature, PPSN XI*, pages 73–82, Berlin, Heidelberg, 2010. Springer Berlin Heidelberg.
- [16] Olaf Mersmann, Bernd Bischl, Heike Trautmann, Mike Preuss, Claus Weihs, and Günter Rudolph. Exploratory landscape analysis. In *Proceedings of the 13th Annual Conference on Genetic and Evolutionary Computation*, GECCO '11, page 829–836, New York, NY, USA, 2011. Association for Computing Machinery.
- [17] Bas van Stein, Hao Wang, and Thomas Bäck. Neural network design: Learning from neural architecture search. In *2020 IEEE Symposium Series on Computational Intelligence (SSCI)*, pages 1341–1349. IEEE, 2020.
- [18] Quentin Renau, Johann Dreo, Carola Doerr, and Benjamin Doerr. Towards explainable exploratory landscape analysis: Extreme feature selection for classifying bbob functions. In Pedro A. Castillo and Juan Luis Jiménez Laredo, editors, *Applications of Evolutionary Computation*, pages 17–33, Cham, 04 2021. Springer International Publishing.
- [19] Fu Xing Long, Bas van Stein, Moritz Frenzel, Peter Krause, Markus Gitterle, and Thomas Bäck. Learning the characteristics of engineering optimization problems with applications in automotive crash. In *Proceedings of the Genetic and Evolutionary Computation Conference*, GECCO '22, page 1227–1236, New York, NY, USA, 2022. Association for Computing Machinery.
- [20] Urban Škvorc, Tome Eftimov, and Peter Korošec. Understanding the problem space in single-objective numerical optimization using exploratory landscape analysis. *Applied Soft Computing*, 90:106138, 2020.
- [21] Quentin Renau, Johann Dreo, Carola Doerr, and Benjamin Doerr. Expressiveness and robustness of landscape features. In *Proceedings of the Genetic and Evolutionary Computation Conference Companion*, GECCO '19, page 2048–2051, New York, NY, USA, 2019. Association for Computing Machinery.
- [22] Moritz Seiler, Janina Pohl, Jakob Bossek, Pascal Kerschke, and Heike Trautmann. Deep learning as a competitive feature-free approach for automated algorithm selection on the traveling salesperson problem, 2020.
- [23] Mario A. Muñoz and Kate A. Smith-Miles. Performance analysis of continuous black-box optimization algorithms via footprints in instance space. *Evol. Comput.*, 25(4):529–554, dec 2017.
- [24] Pascal Kerschke and Heike Trautmann. *Comprehensive Feature-Based Landscape Analysis of Continuous and Constrained Optimization Problems Using the R-Package Flacco*, pages 93–123. Studies in Classification, Data Analysis, and Knowledge Organization. Springer International Publishing, Cham, 2019.
- [25] Pascal Kerschke and Heike Trautmann. flacco: Feature-based landscape analysis of continuous and constrained optimization problems, 2019. Last accessed 15 January 2022.
- [26] Hervé Abdi and Lynne J Williams. Principal component analysis. *Wiley interdisciplinary reviews: computational statistics*, 2(4):433–459, 2010.

- [27] Raphael Patrick Prager, Moritz Vinzent Seiler, Heike Trautmann, and Pascal Kerschke. Automated algorithm selection in single-objective continuous optimization: A comparative study of deep learning and landscape analysis methods. In Günter Rudolph, Anna V. Kononova, Hernán Aguirre, Pascal Kerschke, Gabriela Ochoa, and Tea Tušar, editors, *Parallel Problem Solving from Nature – PPSN XVII*, pages 3–17, Cham, 2022. Springer International Publishing.
- [28] Mohamad Alissa, Kevin Sim, and Emma Hart. Algorithm selection using deep learning without feature extraction. In *Proceedings of the Genetic and Evolutionary Computation Conference, GECCO '19*, page 198–206. Association for Computing Machinery, 2019.
- [29] Moritz Vinzent Seiler, Raphael Patrick Prager, Pascal Kerschke, and Heike Trautmann. A collection of deep learning-based feature-free approaches for characterizing single-objective continuous fitness landscapes, 2022.
- [30] Raphael Patrick Prager, Moritz Vinzent Seiler, Heike Trautmann, and Pascal Kerschke. Towards feature-free automated algorithm selection for single-objective continuous black-box optimization. In *2021 IEEE Symposium Series on Computational Intelligence (SSCI)*, pages 1–8, 2021.
- [31] David Charte, Francisco Charte, María J. del Jesus, and Francisco Herrera. An analysis on the use of autoencoders for representation learning: Fundamentals, learning task case studies, explainability and challenges. *Neurocomputing*, 404:93–107, sep 2020.
- [32] David Charte, Francisco Charte, Salvador García, María J. del Jesus, and Francisco Herrera. A practical tutorial on autoencoders for nonlinear feature fusion: Taxonomy, models, software and guidelines. *Information Fusion*, 44:78–96, nov 2018.
- [33] Yashua Bengio, Aaron Courville, and Pascal Vincent. Representation learning: A review and new perspectives. *IEEE transactions on pattern analysis and machine intelligence*, 35:1798–1828, 08 2013.
- [34] Michael Tschannen, Olivier Bachem, and Mario Lucic. Recent advances in autoencoder-based representation learning, 2018.
- [35] Diederik P. Kingma and Max Welling. Auto-encoding variational bayes. *arXiv preprint arXiv:1312.6114*, 2013.
- [36] Diederik P. Kingma and Max Welling. An introduction to variational autoencoders. *Foundations and Trends® in Machine Learning*, 12(4):307–392, 2019.
- [37] Nikolaus Hansen, Steffen Finck, Raymond Ros, and Anne Auger. Real-Parameter Black-Box Optimization Benchmarking 2009: Noiseless Functions Definitions. Research Report RR-6829, INRIA, 2009.
- [38] Bas van Stein. doe2vec: paper release, September 2022.
- [39] Il'ya Meerovich Sobol'. On the distribution of points in a cube and the approximate evaluation of integrals. *USSR Computational Mathematics and Mathematical Physics*, 7(4):86–112, 1967.
- [40] Ye Tian, Shichen Peng, Xingyi Zhang, Tobias Rodemann, Kay Chen Tan, and Yaochu Jin. A recommender system for metaheuristic algorithms for continuous optimization based on deep recurrent neural networks. *IEEE Transactions on Artificial Intelligence*, 1(1):5–18, 2020.
- [41] Fabian Pedregosa, Gaël Varoquaux, Alexandre Gramfort, Vincent Michel, Bertrand Thirion, Olivier Grisel, Mathieu Blondel, Peter Prettenhofer, Ron Weiss, Vincent Dubourg, Jake Vanderplas, Alexandre Passos, David Cournapeau, Matthieu Brucher, Matthieu Perrot, and Édouard Duchesnay. Scikit-learn: Machine learning in python. *Journal of Machine Learning Research*, 12(85):2825–2830, 2011.